IVA-BASED SPATIO-TEMPORAL DYNAMIC CONNECTIVITY ANALYSIS IN LARGE-SCALE FMRI DATA

Suchita Bhinge[1]*, Vince D. Calhoun*[2,3] *and Tülay Adalı*[1]

[1]Dept. of CSEE, University of Maryland, Baltimore County, MD, 21250
[2]Dept. of ECE, University of New Mexico, Albuquerque, NM, 87131
[3]The Mind Research Network, Albuquerque, NM, 87106

ABSTRACT

Recently, much attention has been devoted to examining time-varying changes in functional connectivity to understand the network structure in the human brain. Most studies, however, analyze the time-varying functional connectivity but ignore the time-varying spatial information. In this paper, we propose a method based on independent vector analysis (IVA) to study dynamic functional network connectivity (dFNC) as well as dynamic spatial functional network connectivity (dsFNC) in fMRI data. Though IVA allows one to effectively capture both, its performance degrades with the increase in the number of datasets. Hence, we propose an effective scheme to bypass this limitation followed by graph theoretical analysis to study both inter-network dynamics and intra-network stationarity. We observe higher dFNC fluctuations for patients with schizophrenia in the default-mode (DM)-salience network and cerebellum with associated connections. dsFNC analysis indicates higher inter-network fluctuation in patients while DM, anterior DM and frontal networks demonstrate significant intra-network fluctuation in controls.

Index Terms— Dynamic functional connectivity, dynamic spatial connectivity, independent vector analysis, network stationarity, temporal graphs

1. INTRODUCTION

The human brain comprises networks that are spatially distributed but functionally associated, continuously interacting with each other. Functional connectivity analysis explores the organization of temporal dependency among these networks and provides a platform to assess the dysfunction in this organization in many cognitive disorders [1]. Studies related to the analysis of functional connectivity are often limited due to an assumption of spatial and temporal stationarity over the scanning period. Recently, many neurological studies have focused on assessing connectivity dynamics to understand the time-varying network structure in healthy controls and in patients with a variety of disorders. These studies have shown changes in the functional connectivity in different stages of hallucination [2] and development [3]. Some of them have also analyzed connectivity dynamics in task-related [4] and resting-state functional magnetic resonance imaging (fMRI) data [5, 6, 7]. However, it has been shown that dynamics is a salient feature at rest-state since rest represents an unconstrained task [8, 9]. In this paper we focus our analysis on resting-state fMRI data.

Most dynamic connectivity analysis methods examine time-varying temporal dependence between brain regions but neglect changes in the spatial networks. A previous study focused only on spatial changes in the default mode (DM) network from healthy individuals using group independent component analysis (ICA) [10]. The only work—to the best of our knowledge—that investigates whole-brain time-varying spatial networks performs independent vector analysis (IVA) using a sliding window approach and investigates networks that demonstrate differences in the time-varying spatial network connectivity between healthy controls and patients with schizophrenia [11]. IVA is a joint blind source separation algorithm that estimates sources that are maximally independent within each dataset while exploiting dependencies across multiple datasets. Unlike other joint blind source separation methods such as group ICA [12], which constrains the spatial networks to be common across subjects and joint ICA [13], which constrains the time courses to be common across subjects, IVA relaxes these assumptions by estimating subject-specific time courses and spatial networks. It has been successfully applied on multi-subject fMRI data and shown superior performance in terms of preserving subject variability as compared to the widely used group ICA method [14, 15], primarily due to this flexibility. However, this flexibility comes at an increased cost as it requires estimation of high-dimensional multivariate probability density functions and as a result performance of IVA degrades as the number of datasets increases. That is potentially a key reason for the fact that the method in [11] is applied to the analysis of only 20 subjects.

In this paper, we propose a novel approach to resolve the high dimensionality issue in IVA by considering pairs of subjects for an IVA decomposition followed by a component alignment step to align the components across IVA decompositions. We also propose to use subject-level graph theoretical (GT) analysis for temporal graphs to study the spatio-temporal connectivity changes. We study the dynamic functional network connectivity (dFNC) and dynamic spatial functional network connectivity (dsFNC) strength and fluctuation along with the intra-network stationarity for two groups of subjects—healthy controls and patients with schizophrenia, and observed higher intra-network dFNC and dsFNC fluctuation in patients and a higher intra-network fluctuation in the DM, anterior DM and frontal networks. The remainder of the paper is organized as follows, Section 2 introduces the general IVA model and component alignment method followed by the description of the proposed method in Section 3. Section 4 introduces the metrics used to study the dynamic spatio-temporal connectivity followed by discussion of the results in Section 5 and Section 6 concludes the paper.

2. BACKGROUND

2.1. Independent vector analysis

IVA is a joint blind source separation technique that extends ICA to multiple datasets, by exploiting statistical dependence across those datasets and statistical independence within each dataset. The general IVA model is given by, $\mathbf{X}^{[k]} = \mathbf{A}^{[k]}\mathbf{S}^{[k]},\ k = 1, \ldots, K$ where $\mathbf{X}^{[k]} \in \mathbb{R}^{T \times V}$ are the observations, $\mathbf{A}^{[k]} \in \mathbb{R}^{T \times T}$ is the mixing ma-

This work was supported in parts by grants NIH-NIBIB R01 EB 020407 and NSF-CCF 1618551.

trix and $\mathbf{S}^{[k]} \in \mathbb{R}^{T\times V}$ is the independent source component matrix for the kth dataset. Here, K is the total number of datasets, V is the number of samples and T is the number of components. The sources are estimated using $\mathbf{Y}^{[k]} = \mathbf{W}^{[k]}\mathbf{X}^{[k]}$, where $\mathbf{W}^{[k]} \in R^{T\times T}$ is the demixing matrix estimated by minimizing the mutual information based cost function given as,

$$\mathcal{J}(\mathcal{W}) = \sum_{t=1}^{T}\left[\sum_{k=1}^{K}\mathcal{H}\left(y_t^{[k]}\right) - \mathcal{I}\left(\mathbf{y}_t\right)\right] - \sum_{k=1}^{K}\log\left|\det\left(\mathbf{W}^{[k]}\right)\right|,$$

where $\mathbf{y}_t = \left[\mathbf{y}_t^{[1]}, \ldots, \mathbf{y}_t^{[K]}\right]^T$ denotes the tth SCV, which is defined by concatenating the nth source from each dataset. Minimization of the cost function equally weights the minimization of estimated source entropy, $\mathcal{H}\left(y_t^{[k]}\right)$ and maximization of the dependence within the tth SCV, $\mathcal{I}\left(\mathbf{y}_t\right)$, thus, grouping together similar components across datasets in one SCV.

A number of IVA algorithms have been proposed based on different models for the source distribution, *e.g.*, multivariate Gaussian (IVA-G) [16], which exploits only second order statistics through a covariance matrix of each SCV, $\Sigma_t \in \mathbb{R}^{K\times K}$ and multivariate Laplace (IVA-L) [17], which exploits higher order statistics. In this paper we use IVA-GL, an IVA algorithm that initializes IVA-L using the IVA-G result, since it has been shown to be an effective and efficient way to include all-order statistical information [16]. However, even within this structure, the covariance matrices in IVA-G require the estimation of $T\left(K(K-1)/2\right)$ parameters since each matrix is symmetric, in addition to the estimation of approximately KT^2 parameters for the demixing matrices that increase rapidly with increase in the number of datasets. Thus for a fixed number of samples, the estimation of the parameters deteriorates for large K degrading the performance of IVA. Hence, we propose a procedure that divides the datasets into smaller subsets to perform IVA on each subset.

3. SUBSET IVA FOR SPATIO-TEMPORAL DYNAMIC CONNECTIVITY ANALYSIS

In order to study the spatio-temporal connectivity changes in resting-state fMRI data we propose a three step procedure: two-subject IVA using sliding window, component alignment, and component clustering, as shown in Figure 1.

3.1. Two-subject IVA using sliding window

In this stage, we first partition each subject's data into M time windows using a sliding window of length L. The data from the kth subject and mth window forms a dataset, $\mathbf{X}^{[m,k]}, m = 1, \ldots, M,\ k = 1, \ldots, K$ yielding a total of MK datasets, which can be decomposed into MK mixing matrices, $\mathbf{A}^{[m,k]} \in \mathbb{R}^{L\times N}$, whose columns represent the time courses and MK source matrices, $\mathbf{S}^{[m,k]} \in \mathbb{R}^{N\times V}$, whose rows represent independent spatial networks. However, due to the dimensionality issue, we consider time windows from two subjects in each IVA decomposition yielding $P = K/2$ unique IVA decompositions, and estimate $2M$ demixing matrices followed by estimation of the underlying sources, $\mathbf{Y}^{[m,k]} = \mathbf{W}^{[m,k]}\widehat{\mathbf{X}}^{[m,k]},\ m = 1, \ldots, M,\ k = \{k_1, k_2\}$ and $\mathbf{Y}^{[m,k]} \in \mathbb{R}^{N\times V}, \widehat{\mathbf{X}}^{[m,k]} \in \mathbb{R}^{N\times V}, \mathbf{W}^{[m,k]} \in \mathbb{R}^{N\times N}$. $\widehat{\mathbf{X}}^{[m,k]}$ are the first N principal components of $\mathbf{X}^{[m,k]}$ and $\{k_1, k_2\}$ are unique pairwise combinations of K datasets.

3.2. Component alignment

Due to an inherent permutation ambiguity in ICA, the estimated SCVs across multiple IVA decompositions are not aligned. Thus, to align the components across all IVA decompositions, we use the linear assignment problem (LAP) [18]. Instead of aligning N components from MK datasets, we minimize our problem by computing an average across $2M$ windows in each SCV, $\bar{\mathbf{y}}_n^{(p)}$, thus yielding N mean components for P decompositions. A distance matrix, $\mathbf{D}^{(p_1,p_2)}$ is calculated for each decomposition pair, where each element is given by, $d_{n_1,n_2} = 1 - \mathcal{I}(\bar{\mathbf{y}}_{n_1}^{(p_1,p_2)}, \bar{\mathbf{y}}_{n_2}^{(p_1,p_2)}),\ n_1, n_2 \in \{1, \ldots, N\},\ p_1, p_2 \in \{1, \ldots, P\}$. $\mathcal{I}(\cdot)$ denotes the normalized mutual information operator defined in (2). We obtain the minimum cost of assigning the components using the Hungarian algorithm [19] followed by a weighted graph with P nodes and edges as the minimum cost of LAP. A central node is computed using an MST by finding the minimum cost sub-graph connecting all nodes and the components in each decomposition are aligned as per the central node.

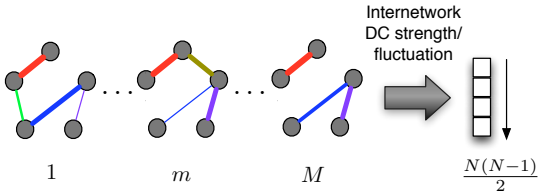

Fig. 2. A temporal graph of 5 nodes at M time instances. A thick edge represents higher connection between the corresponding nodes and vice-versa. For each pair of nodes, we compute the average connectivity strength and connectivity fluctuation.

3.3. Component clustering

The component alignment step aligns the mean components, $\mathbf{y}_n,\ n = 1, \ldots, N$, across P subject pairs such that $\bar{\mathbf{y}}_n^{(p)}$ for all $p \in \{1, \ldots, P\}$ represent similar networks. However, since real data does not follow the IVA model exactly, some components are not estimated consistently and are mis-aligned in the component alignment step, as shown in Figure 1. In order to remove the mis-aligned components from further analysis, we perform hierarchical clustering to cluster the aligned components in one cluster and the misaligned components in a different cluster. A dendrogram is used to visualize the hierarchy of clusters with a correlation threshold of c used to separate two clusters, *i.e.*, if the correlation between two clusters is greater than c then the two clusters are merged to form one cluster. The cluster that includes highest number of decomposition pairs is denoted as the aligned cluster and used for further analysis.

4. DYNAMIC CONNECTIVITY METRICS

4.1. Inter-network dynamic connectivity analysis

We use GT analysis defined for temporal graphs [20] to summarize the connectivity changes in the time-varying functional and spatial networks. For each subject, we obtain two temporal graphs using time courses and spatial maps, each formed from a set of N nodes and $N(N-1)/2$ edges for each time window, as shown in Figure 2. We define an edge between two time courses using the absolute value of Pearson's correlation coefficient and an edge between two spatial components using the normalized mutual information defined in 2. Let an edge between node n_1 and n_2 at time interval m be denoted as $a_{n_1n_2}(m), m = 1, \ldots, M,\ n_1, n_2 = \{1, \ldots, N\}$. The inter-network connectivity strength between node n_1 and n_2 between time interval m and $m+1$ is defined as follows [20],

$$C_{n_1n_2}(m, m+1) = \frac{a_{n_1n_2}(m)a_{n_1n_2}(m+1)}{\sqrt{\left[a_{n_1n_2}(m)\right]\left[a_{n_1n_2}(m+1)\right]}}, \quad (1)$$

where $\{n_1, n_2\}$ represent all unique pairs and $m = 1, \ldots, M-1$. The inter-network dynamic connectivity strength is thus obtained as,

$$\bar{C}_{n_1n_2} = \frac{1}{M-1}\sum_{m=1}^{M-1} C_{ij}(m, m+1).$$

A higher value of $\bar{C}_{n_1n_2}$ indicates higher dynamic connectivity strength between nodes n_1 and n_2. The inter-network dynamic con-

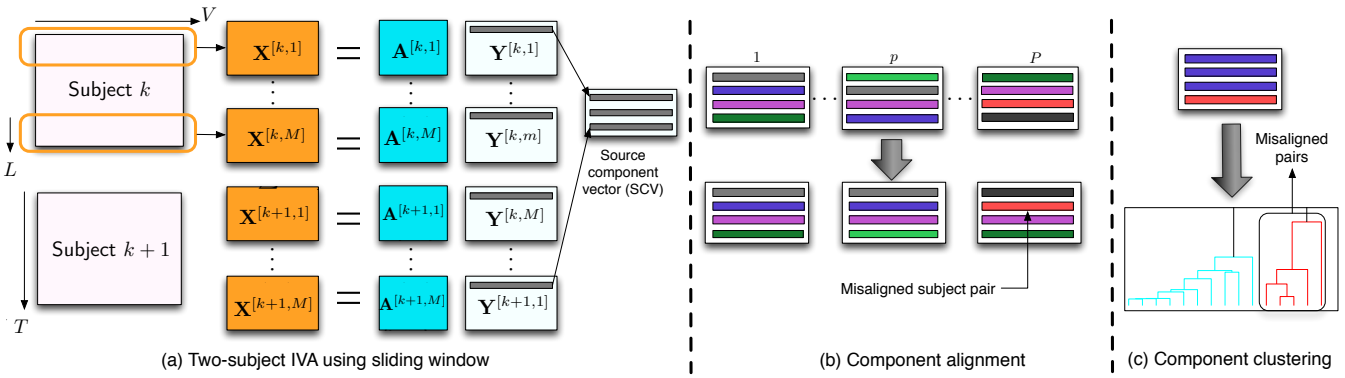

Fig. 1. Proposed three-stage method: (a) two-subject IVA using a sliding window (b) component alignment and (c) component clustering.

nectivity fluctuation between two nodes n_1 and n_2 by computing the standard deviation of (1) across all windows. This metric measure the variability of the inter-network connectivity across time instants.

4.2. Intra-network stationarity

In order to study the fluctuations in the activation in the spatial network across time windows, we use normalized mutual information, which is defined as follows,

$$\mathcal{I}\left(\mathbf{y}_n^{[m,k]}, \mathbf{y}_n^{[m+1,k]}\right) = \frac{2 * I\left(\mathbf{y}_n^{[m,k]}, \mathbf{y}_n^{[m+1,k]}\right)}{I\left(\mathbf{y}_n^{[m,k]}, \mathbf{y}_n^{[m,k]}\right) + I(\mathbf{y}_n^{[m+1,k]}, \mathbf{y}_n^{[m+1,k]})}, \quad (2)$$

where $I(\cdot)$ denotes the non-normalized mutual information obtained using [21]. We then define the intra-network stationarity metric as,

$$\bar{\mathcal{I}}_n^{[k]} = \frac{1}{M-1} \sum_{m=1}^{M-1} \mathcal{I}\left(\mathbf{y}_n^{[m,k]}, \mathbf{y}_n^{[m+1,k]}\right), n = 1, \ldots, N$$

Thus $\bar{\mathcal{I}}_n^{[k]}$ indicates the level of stationarity, where 0 indicates the network activation is highly variable and 1 indicates it is stable.

5. RESULTS

We apply the proposed method on a dataset from the Center for Biomedical Research Excellence (COBRE) (http://coins.mrn.org/dx) [22] that consist of 90 healthy controls (HCs) (average age: 38 ± 12) and 88 patients with schizophrenia (SZs) (average age: 37 ± 14) obtained during rest with their eyes open. The fMRI image scans were collected using a 3-Tesla Siemens scanner over an interval of 300 seconds with a sampling period of 2 seconds yielding 150 timepoints per subject. The first 6 timepoints are removed due to an observed T1-effect. Each subject's image data is then pre-processed for re-alignment, slice-time correction, spatial normalization and re-sampled to $3 \times 3 \times 3\text{mm}^3$ giving $53 \times 63 \times 46$ voxels. Masking on each image volume is performed on to remove the non-brain voxels and flattened to form an observation vector of $V = 58604$ samples, giving $T = 144$ observations for each subject. Each dataset is partitioned into $M = 19$ windows of length $L = 36$ with an overlap of 30 time points between adjacent time windows.

After partitioning each subject's data, we select two unique subjects from either SZs or HCs for an IVA decomposition, hence we have a total of $P = 89$ (45 HC pairs + 44 SZ pairs) IVA decompositions. We obtain 10 independent solutions of $\mathbf{W}^{[m,k]}$ using IVA-GL and obtain the best solution using MST approach proposed in [23]. We estimate $N = L = 36$ components in each IVA decomposition followed by component alignment and clustering to remove the misaligned subject pairs. We obtain a dendrogram for each component after alignment using a threshold of $c = 0.2$ to visualize the clustering. An example of the dendrogram obtained for the parietal component in shown in Figure 3. A low threshold is considered to account for subject variability. The dendrograms for most components show clear clustering for the aligned and misaligned subject pairs as in Figure 3. Since dsFNC and dFNC analysis is between any two components, the misaligned subject pairs for both corresponding components are removed, while for average mutual information only the misaligned subject pairs for that component are removed. Thus, for each component, the remainder dataset consists of subjects in the range 126 to 176, with 47% to 52% HCs, indicating enough samples in each group.

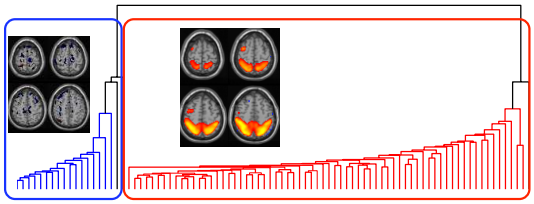

Fig. 3. Dendrogram of parietal component. The spatial maps represents the significant activation areas across the subject pairs in the corresponding cluster, obtained using one-sample t-test. Red cluster includes the perfectly aligned subject pairs while the blue cluster includes the misaligned subject pairs.

After alignment and clustering, we perform component selection to select the components of interest since some of the estimated IVA components show activation in the brainstem nuclei and some are motion artifacts. Of the 36 components, we select 15 functionally relevant components based on visual inspection and clustering, since these components yield tightly packed clusters unlike the noise components, which yield multiple uncorrelated clusters. For each selected component, we perform a one-sample t-test on each voxel across all the aligned mean components to generate t-statistic map, which represents the significantly activated region across all subject pairs [24]. The t-statistic maps of the selected components are shown in Figure 4.

5.1. Inter-network dynamic connectivity analysis

We compute inter-network dynamic connectivity strength and fluctuation using time courses and spatial networks for all the pairwise combination of the selected components, *i.e.*, 105 distinct combinations. We then compute a two-sample t-test and Mann-Whitney U-test on dynamic connectivity strength and dynamic connectivity fluctuation respectively, in order to find edges that demonstrate significant difference between two groups. The edges that demonstrated

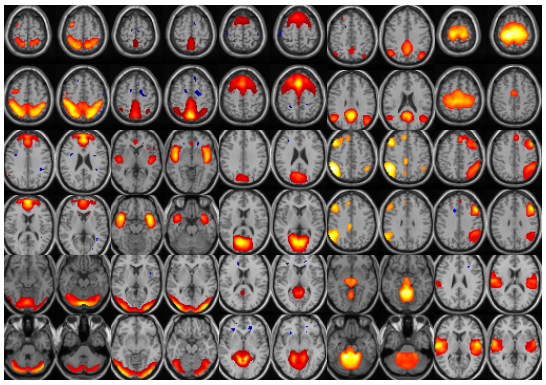

Fig. 4. Of the 36 estimated components, we select 15 functionally relevant components for dynamic connectivity and intra-network stationarity analysis.

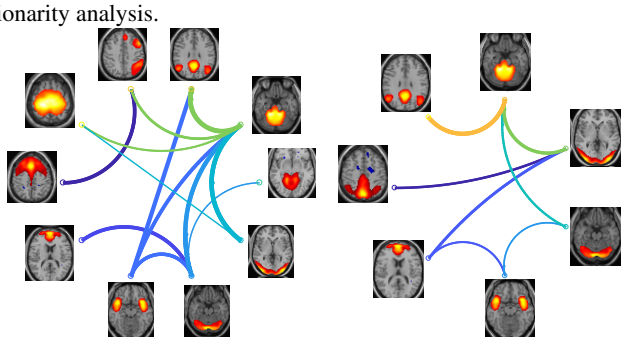

(a) (b)

Fig. 5. (a) All network pairs indicate higher inter-network dynamic connectivity strength in patients using time courses. (b) All network pairs except the parietal-visual connection show higher inter-network dynamic connectivity fluctuation in patients using time courses.

significant ($p < 0.05$, false discovery rate (FDR) corrected) difference between the two groups using time courses and spatial networks are shown in Figure 5 and 6 respectively. Each node in Figure 5 and 6 denotes a spatial network or time course while the edge connecting them denotes the level of discrimination between HCs and SZs. A thick line represents a lower p-value, *i.e.*, higher discrimination between the two groups and vice-versa.

Consistent results are observed using the dynamic connectivity strength using time course and spatial networks in the DM-insular connectivity. Our results indicate higher dFNC and dsFNC strength in patients in the DM-insular conectivity and higher fluctuation in the dsFNC is observed in patients. Similar results were observed in [25], in which higher connectivity strength is observed among DM and the salience network, whose prominant node lies in the insular region, in patients. The study also shows no significant difference in the fluctuation of the dFNC in this network pair. This study also shows higher strength in the DM-central executive network (frontoparietal region) which is also observed in the dsFNC analysis. Studies have shown aberrant connectivity between cerebellar and associated network, indicating its importance in the pathophysiology of schizophrenia. Higher dFNC strength is observed between cerebellar and associated functional networks, especially among the DM-cerebellum region, which is consistent with the findings in [26].

5.2. Intra-network stationarity

We also compute intra-network stationarity metric for all selected components after removing the misaligned subject pairs. We compute a two-sample t-test on each component's values to test for differences between HCs and SZs. The boxplots for the networks that demonstrated significant ($p < 0.05$, FDR corrected) group difference between HC and SZ groups are shown in Figure 7. Higher network fluctuation is observed HCs when compared with SZs in the DM, anterior DM and frontal regions of the brain. Similar results were observed in [11], where the authors noted that DM tends to fluctuate between states in HCs when compared with SZs.

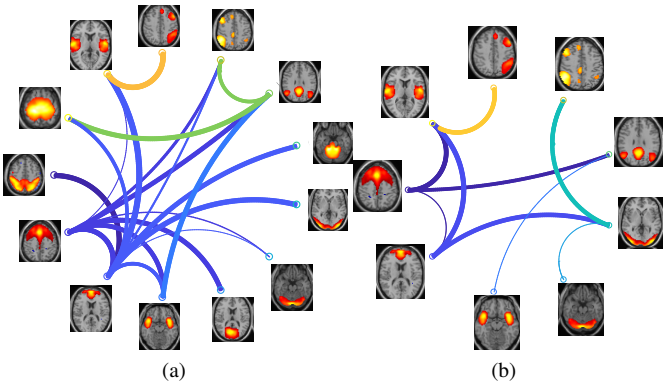

(a) (b)

Fig. 6. (a) All network pairs indicate higher inter-network dynamic connectivity strength in patients using spatial networks. (b) All network pairs indicate higher inter-network dynamic connectivity fluctuation in patients using spatial networks.

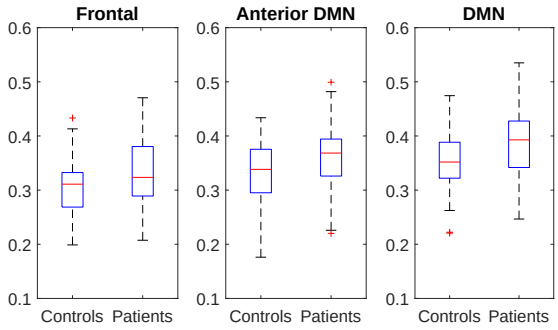

Fig. 7. Intra-network stationarity for the components that demonstrated significant ($p < 0.05$) difference between HCs and SZs. The read line is the median, top and bottom edges of the blue box is the 25th and 75th percentile, the dotted line extends from maximum to minimum and '+' denotes the outliers.

6. CONCLUSION

In this paper, we proposed a method to analyze the spatio-temporal connectivity changes in rest-state fMRI data and show that dFNC and dsFNC are both prominant features to distinguish the underlying structure of the brain in healthy controls and in patients with schizophrenia. In general, we observe higher inter-network dynamic connectivity fluctuation in patients, which is justified since patients with schizophrenia are known to have abnormal connectivity/dysconnectivity pattern. Higher inter-network dynamic connectivity fluctuations are observed in patients with schizophrenia among the DM-salience network, DM-LFP, anterior DM-associated network and cerebellar-associated networks. Intra-network connectivity analysis indicates higher fluctuation in the DM, anterior DM and frontal region in controls when compared with patients. The success of the proposed method suggests further studies to evaluate the robustness under variable sliding window lengths to vary the temporal resolution.

7. REFERENCES

[1] A. Aertsen, G. Gerstein, M. Habib, and G. Palm, "Dynamics of neuronal firing correlation: modulation of 'effective connectivity'," *Journal of Neurophysiology*, vol. 61, no. 5, pp. 900–917, 1989.

[2] S. Lefebvre, M. Demeulemeester, A. Leroy, C. Delmaire, R. Lopes, D. Pins, P. Thomas, and R. Jardri, "Network dynamics during the different stages of hallucinations in schizophrenia," *Human Brain Mapping*, vol. 37, no. 7, pp. 2571–2586, 2016.

[3] L. Q. Uddin, K. S. Supekar, S. Ryali, and V. Menon, "Dynamic reconfiguration of structural and functional connectivity across core neurocognitive brain networks with development," *Journal of Neuroscience*, vol. 31, no. 50, pp. 18 578–18 589, 2011.

[4] Ü. Sakoğlu, G. D. Pearlson, K. A. Kiehl, Y. M. Wang, A. M. Michael, and V. D. Calhoun, "A method for evaluating dynamic functional network connectivity and task-modulation: application to schizophrenia," *Magnetic Resonance Materials in Physics, Biology and Medicine*, vol. 23, no. 5-6, pp. 351–366, 2010.

[5] X. Di and B. B. Biswal, "Dynamic brain functional connectivity modulated by resting-state networks," *Brain Structure and Function*, vol. 220, no. 1, pp. 37–46, 2015.

[6] E. A. Allen, E. Damaraju, S. M. Plis, E. B. Erhardt, T. Eichele, and V. D. Calhoun, "Tracking whole-brain connectivity dynamics in the resting state," *Cerebral Cortex*, vol. 24, no. 3, pp. 663–676, 2014.

[7] E. Damaraju, E. Allen, A. Belger, J. Ford, S. McEwen, D. Mathalon, B. Mueller, G. Pearlson, S. Potkin, A. Preda *et al.*, "Dynamic functional connectivity analysis reveals transient states of dysconnectivity in schizophrenia," *NeuroImage: Clinical*, vol. 5, pp. 298–308, 2014.

[8] G. Deco, A. Ponce-Alvarez, D. Mantini, G. L. Romani, P. Hagmann, and M. Corbetta, "Resting-state functional connectivity emerges from structurally and dynamically shaped slow linear fluctuations," *Journal of Neuroscience*, vol. 33, no. 27, pp. 11 239–11 252, 2013.

[9] P. Delamillieure, G. Doucet, B. Mazoyer, M.-R. Turbelin, N. Delcroix, E. Mellet, L. Zago, F. Crivello, L. Petit, N. Tzourio-Mazoyer *et al.*, "The resting state questionnaire: an introspective questionnaire for evaluation of inner experience during the conscious resting state," *Brain Research Bulletin*, vol. 81, no. 6, pp. 565–573, 2010.

[10] V. Kiviniemi, T. Vire, J. Remes, A. A. Elseoud, T. Starck, O. Tervonen, and J. Nikkinen, "A sliding time-window ica reveals spatial variability of the default mode network in time," *Brain Connectivity*, vol. 1, no. 4, pp. 339–347, 2011.

[11] S. Ma, V. D. Calhoun, R. Phlypo, and T. Adalı, "Dynamic changes of spatial functional network connectivity in healthy individuals and schizophrenia patients using independent vector analysis," *NeuroImage*, vol. 90, pp. 196–206, 2014.

[12] V. D. Calhoun, T. Adalı, G. D. Pearlson, and J. Pekar, "A method for making group inferences from functional MRI data using independent component analysis," *Human Brain Mapping*, vol. 14, no. 3, pp. 140–151, 2001.

[13] T. Adalı, Y. Levin-Schwartz, and V. D. Calhoun, "Multimodal data fusion using source separation: Two effective models based on ICA and IVA and their properties," *Proceedings of the IEEE*, vol. 103, no. 9, pp. 1478–1493, 2015.

[14] A. M. Michael, M. Anderson, R. L. Miller, T. Adalı, and V. D. Calhoun, "Preserving subject variability in group fMRI analysis: performance evaluation of GICA vs. IVA," *Frontiers in Systems Neuroscience*, vol. 8, 2014.

[15] J.-H. Lee, T.-W. Lee, F. A. Jolesz, and S.-S. Yoo, "Independent vector analysis (IVA): multivariate approach for fMRI group study," *NeuroImage*, vol. 40, no. 1, pp. 86–109, 2008.

[16] M. Anderson, T. Adalı, and X.-L. Li, "Joint blind source separation with multivariate Gaussian model: Algorithms and performance analysis," *IEEE Transactions on Signal Processing*, vol. 60, no. 4, pp. 1672–1683, April 2012.

[17] T. Kim, T. Eltoft, and T.-W. Lee, "Independent vector analysis: An extension of ICA to multivariate components," in *Independent Component Analysis and Blind Signal Separation*, ser. Lecture Notes in Computer Science. Berlin, Germany: Springer, 2006, vol. 3889, pp. 165–172.

[18] T. C. Koopmans and M. Beckmann, "Assignment problems and the location of economic activities," *Econometrica: Journal of the Econometric Society*, pp. 53–76, 1957.

[19] H. W. Kuhn, "The Hungarian method for the assignment problem," *Naval Research Logistics (NRL)*, vol. 2, no. 1-2, pp. 83–97, 1955.

[20] V. Nicosia, J. Tang, C. Mascolo, M. Musolesi, G. Russo, and V. Latora, "Graph metrics for temporal networks," in *Temporal networks*. Springer, 2013, pp. 15–40.

[21] H. Peng, F. Long, and C. Ding, "Feature selection based on mutual information criteria of max-dependency, max-relevance, and min-redundancy," *IEEE Transactions on Pattern Analysis and Machine Intelligence*, vol. 27, no. 8, pp. 1226–1238, 2005.

[22] A. Scott, W. Courtney, D. Wood, R. De la Garza, S. Lane, R. Wang, M. King, J. Roberts, J. A. Turner, and V. D. Calhoun, "Coins: an innovative informatics and neuroimaging tool suite built for large heterogeneous datasets," *Frontiers in Neuroinformatics*, vol. 5, p. 33, 2011.

[23] W. Du, S. Ma, G.-S. Fu, V. D. Calhoun, and T. Adalı, "A novel approach for assessing reliability of ICA for fMRI analysis," in *IEEE International Conference on Acoustics, Speech and Signal Processing (ICASSP)*, Florence, Italy, 2014, pp. 2084 – 2088.

[24] V. D. Calhoun and T. Adalı, "Multisubject independent component analysis of fMRI: A decade of intrinsic networks, default mode, and neurodiagnostic discovery," *IEEE Reviews in Biomedical Engineering*, vol. 5, pp. 60–73, 2012.

[25] X. Wang, W. Zhang, Y. Sun, M. Hu, and A. Chen, "Aberrant intra-salience network dynamic functional connectivity impairs large-scale network interactions in schizophrenia," *Neuropsychologia*, vol. 93, pp. 262–270, 2016.

[26] A. K. Shinn, J. T. Baker, K. E. Lewandowski, D. Öngür, and B. M. Cohen, "Aberrant cerebellar connectivity in motor and association networks in schizophrenia," *Frontiers in Human Neuroscience*, vol. 9, 2015.